Desalination and Water Treatment
www.deswater.com
43 (2012) 221–229
April

doi: 10.1080/19443994.2012.672175

Taylor & Francis
Taylor & Francis Group

Fabrication and characterization of the chlorine-tolerant disulfonated poly(arylene ether sulfone)/hyperbranched aromatic polyamide-grafted silica composite reverse osmosis membrane

Si Young Park, Sang Gon Kim, Jeong Hwan Chun, Byung-Hee Chun, Sung Hyun Kim*

Department of Chemical & Biological Engineering, Korea University, 1, 5-Ga, Anam-Dong, Sungbuk-Gu, Seoul 136-713, South Korea
Tel. +82 2 3290 3297; Fax: +82 2 926 6102; email: kimsh@korea.ac.kr

Received 25 December 2011; Accepted 10 February 2012

ABSTRACT

In this study, hyperbranched aromatic polyamide-grafted silica (HBP-g-silica) and disulfonated 4,4-bis(3-aminophenoxy)phenyl sulfone (aPES) composite membrane was prepared to enhance the chlorination resistance of reverse osmosis (RO) membrane for desalination process. As the commercial polyamide (PA) RO membrane is very weak against free chlorine in desalination process, inorganic nanoparticle and new membrane material were introduced to RO membrane's active layer. The HBP-g-silica which includes lots of PA chains on the surface of silica and the new material aPES for RO membrane were characterized by ^{1}H-NMR and Fourier transform infrared spectroscopy (FT-IR). The surface morphology of synthesized RO membrane was characterized by scanning electron microscope, and the performance, salt rejection, and water flux were evaluated before and after chlorination test. After the chlorination test, salt rejection was decreased by 36.2% and water permeation was increased only by 5.6% compared to the performance before chlorination measurement. The HBP-g-silica loading significantly modified the three-dimensional polyamide network structures and contributed to high performance by the chain stiffness of the copolymer with high degree of cross-linking. Therefore, the HBP-g-silica that protects PA structure from degradation enhances chlorine resistance in RO membrane.

Keywords: HBP-g-silica; aPES; Chlorine resistance; Reverse osmosis membrane

1. Introduction

In the past several years, there has been increasing interest in RO membrane for desalination [1]. Thin-film composite (TFC) polyamide (PA) membranes are currently used in commercial RO membranes [2]. The active layer of these membranes is formed by interfacial polymerization on top of mesoporous ultrafiltration (UF) support layer. The interfacial polymerization is based on a polycondensation reaction between polyfunctional amine and acid chloride. Among these materials, m-phenylenediamine (MPD) and trimesoyl chloride (TMC) are the most successful commercial products [3,4]. Water flux and salt rejection rate are two key parameters for RO membranes. Ideally, RO membranes should possess high flux and high salt rejection, in addition to excellent chlorine

*Corresponding author.

and fouling resistance, mechanical durability, and low cost. However, PA membranes have some drawbacks such as chlorine susceptibility in the desalination process [5]. The research has been carried out to develop chlorine resistance membranes with higher salt rejection, water permeation through changing monomer structure [6–8], adding nanoparticle [9,10], and design and synthesis of new polymer membranes [11,12].

Sulfonated poly arylene ether sulfones (PESs) based on polysulfone have excellent chemical, mechanical properties, and thermal stability. PESs do not possess the vulnerable amide bond that is susceptible to chlorine attack. However, the salt rejection is below the acceptable level necessary for commercialization [13]. The use of sulfonated aromatic polymers as RO membranes began with sulfonated poly phenyleneoxide in the 1970s [14]. PES membranes have also been considered for RO applications [15,16]. The early success of McGrath in using sulfonated aromatic polymers as RO membrane has led to intensive research [17]. However, all of these membranes were postsulfonated using concentrated sulfuric acid, and undesirable side reactions and poor quantitative reproducibility were encountered. Paul et al. characterized the membrane via a series of controlled molecular weight which disulfonated 50% of PES with phenoxide endgroups [18].

Introduction of hyperbranched aromatic polyamide-grafted silica (HBP-g-silica), which includes lots of amine groups on the surface of silica, can enhance the chlorination resistance of PA membrane for desalination process. Amine groups on the surface of silica particles are chemically combined with copolymer in the PA active membrane and change the matrix of active layer into firm and complex structure with steric conformation. In this study, an enhanced chlorine-tolerant TFC RO membrane was prepared by introducing aPES and HBP-g-silica. Furthermore, the surface-modified nanoparticles were synthesized to enhance the effect of nanopaticles in RO membrane active layer. TFC membrane was prepared through an interfacial polymerization on the polysulfone supporting film. The characterization of synthesized HBP-g-silica, chemical structure of polymer, morphology of the TFC membrane, as well as the chlorine resistance was also discussed. To evaluate the influence of the aPES and HBP-g-silica in the modified membrane, water permeation and salt rejection were measured before and after exposure in a solution of 500 mg/L aqueous sodium hypochlorite (NaOCl) for 24 h at room temperature for accelerated stress test of RO membrane. All tests were conducted at 55 bar and room temperature using a 32 g/L NaCl solution of the same condition with desalination process in the cross-flow cell apparatus.

2. Experimental

2.1. Chemicals

Nano-sized silica with an average diameter of 7 nm, 1,3-aminopropyl triethoxysilane (APS), 3,5-diaminobenzoic acid (DABA), 4-(4,6-dimethoxy-1,3,5-triazine-2-yl)-4-4-methyl-morpholinium chloride (DMTMM) were purchased from Aldrich, Seoul, Korea. The disulfonated material was synthesized with 3-amino phenol, sulfonated 4,4′-dichlorodiphenyl-sulfone (SDCDPS), potassium carbonate (K_2CO_3) which were obtained from Aldrich, Seoul, Korea. These monomers were used as received. The materials, MPD, triethylamine (TEA) in distilled water as aqueous phase and TMC in cyclohexane as organic phase were obtained from Aldrich, Seoul, Korea. The solvents, toluene, methanol, ethanol, dimethylacetamide (DMAc) were of analytical grade purchased from TCI, Korea and were used without further purification.

2.2. Synthesis of aPES

The aPES was synthesized by the method of McGrath et al. [19–21]. A mixture of 6.65 g 3-amino phenol, 9.27 g dry K_2CO_3, 90 ml of dry DMAc, and 37.5 ml of toluene was stirred by refluxing at 145°C for 6 h. Fifteen grams of SDCDPS was added into the mixture along with 15 ml of more DMAc and the reaction mixture was stirred by heating at 170°C for 20 h. The reaction solution was filtered to remove the salt and then cooled down to room temperature. The synthesized aPES was isolated by precipitating in ethyl acetate solution resulting in very light brown solid.

2.3. Synthesis of HBP-g-silica

The following experimental procedures were applied for the synthesis of HBP-g-silica. A mixture of 5.0 g nano-silica, 150 mL toluene, and 5 g APS was stirred under refluxing temperature for 8 h under nitrogen atmosphere. The APS-silica particles were filtered and extracted with ethanol for 24 h to remove the excess silane adsorbed on the silica. After, the light brown powder was dried overnight at 60°C under vacuum. A mixture of 5.0 g APS-silica, 15.2 g DABA, 2.76 g DMTMM, and 500 ml methanol was stirred for 24 h at room temperature under nitrogen atmosphere. The

HBP-g-silica product was filtered and extracted with methanol for 12 h. Finally, the HBP-g-silica was washed with methanol and was dried overnight at 60°C under vacuum.

2.4. Fabrication of TMC membrane

The composite RO membranes were prepared using the following procedure. The porous polysulfone UF membranes (UE50, Trisep Corporation, USA) were used as a support membrane. The types of RO membranes which were polyamide membrane (PAM), aPES composite polyamide membrane (aPAM), and HBP-g-silica/aPES composite polyamide membrane (H-aPAM) were fabricated by interfacial polymerization. Fig. 1 shows that chemical structure of RO membranes (a) PAM, (b) aPAM, and (c) H-aPAM. First, 1 wt% aqueous solution was prepared by the dilution of TEA in distilled water. The 1 wt% aqueous solution was poured over the support membrane and allowed to soak in for 2 min. The excess solution was drained from the surface by soft rubber roller until no liquid had remained. The membrane was placed into an organic phase solution of 0.1 wt% TMC in cyclohexane for 1 min. After removing the excess organic phase solution, the membrane was heated in an oven at 60° C for 1 min. The optimal ratio of aPES to MPD and inorganic particle contents in RO membrane were obtained by other researches in our laboratory. Table 1 described the fabrication type of RO membranes and mixture component of aqueous phase solution.

2.5. Membrane performance evaluation

All tests were conducted at 55 bar and room temperature using a 32 g/L NaCl solution in the cross-flow cell apparatus. The chlorine resistance of RO membrane was evaluated comparing the salt rejection

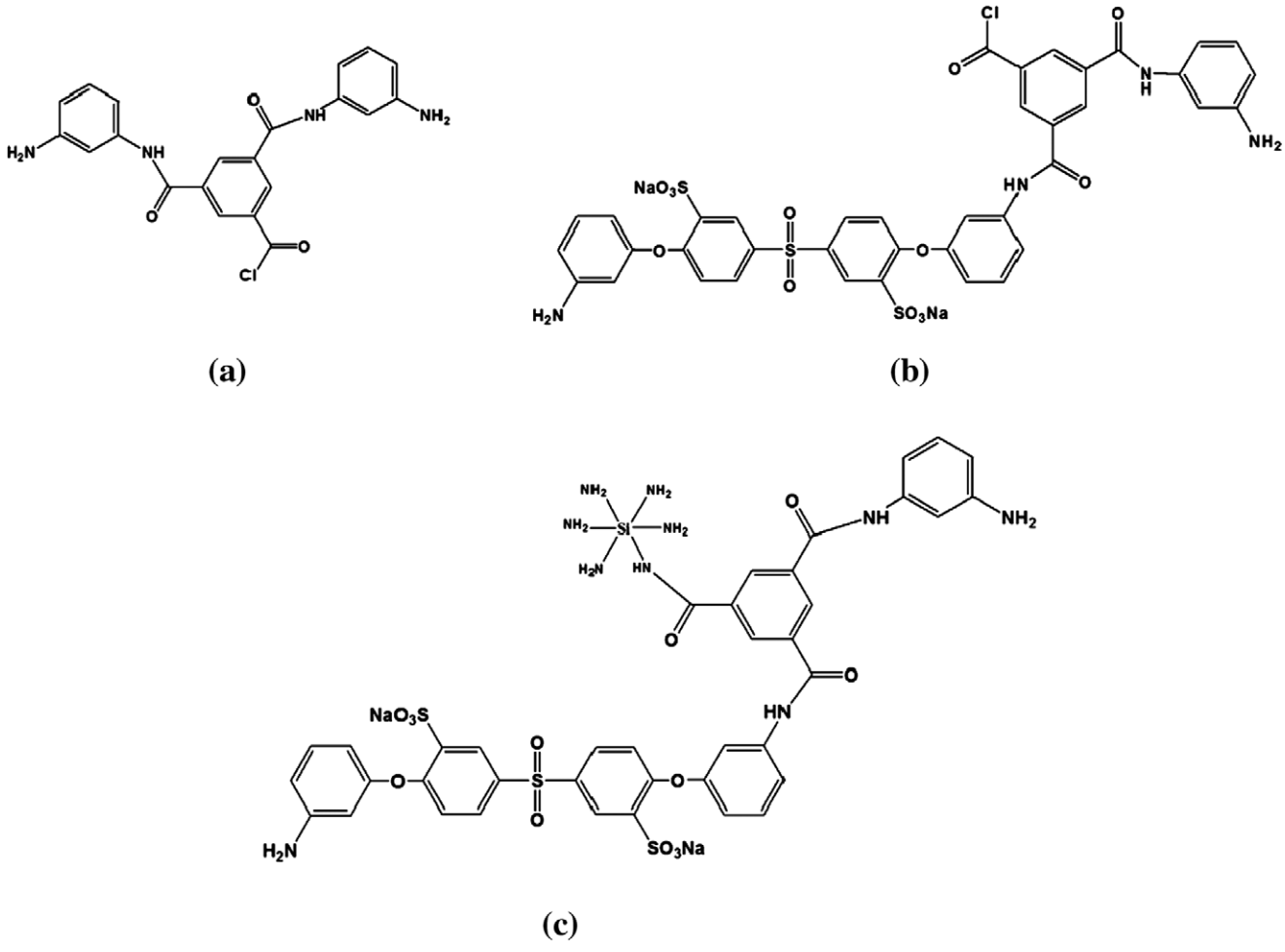

Fig. 1. Chemical structure of RO membranes: (a) PAM, (b) aPAM, and (c) H-aPAM.

Table 1
Fabrication type of RO membranes and mixture component of aqueous phase solution

Membrane	Polyfunctional amine	Inorganic particle
PAM	MPD	–
aPAM	aPES:MPD (1:1)	–
H-aPAM	aPES:MPD (1:1)	HBP-g-silica 2 wt%

and water permeation before and after hypochlorite exposure with 500 mg/L NaOCl solution for 24 h at room temperature. Synthesized RO membranes were soaked in chlorine solution for hypochlorite exposure. The area of effective membrane was around 12.56 cm^2. The water flux was measured by the amount of water permeation flow in terms of liter per square meter-hour ($L/m^2 h$). The salt rejection rate was determined by the salt concentration in the feed solution (C_f) and permeate solution (C_p) obtained by a conductivity meter (PC 650, EUTECH) and was calculated by using the following equation:

$$\text{rejection}(\%) = \left(\frac{C_f - C_p}{C_f}\right) \times 100$$

2.6. Characterization

The molecular structure of aPES was identified by elemental analysis such as C, H, N. ^{1}H-nuclear magnetic resonance (NMR) spectra of the products were obtained at 300 MHz on the Varian Mercury 300 spectrometer using dimethyl sulfoxide-d_6 (DMSO-d_6) as a solvent. The characterization of synthesized HBP-g-silica and composite polymer on the RO membrane was identified by Fourier transform infrared spectroscopy (FT-IR). The FT-IR spectra were recorded by using a Bomen DA-8 spectrometer. The membrane surface was imaged by a scanning electron microscope (SEM) with an S-4300, Hitachi, Japan.

3. Results and discussion

3.1. Synthesis and characterization of aPES

The aPES was synthesized via aromatic nucleophilic reaction chemistry using SDCDPS intermediate and m-aminophenol as a nucleophile in the presence of K_2CO_3. The molecular structure and composition of the aPES were confirmed by proton ^{1}H-NMR in DMSO-d_6. The ^{1}H-NMR spectra show seven different aromatic ring protons that appear at H1 (8.21 ppm), H2 (7.79 ppm), H3 (7.0 ppm), H4 and H5 (6.19 ppm), H6 (6.88 ppm), and H7 (6.39 ppm) Fig. 2. Aromatic amine proton shows a peak at 5.33 ppm which means the amine functional group in the sulfonated poly (arylene ether sulfone) material. The protons have an integration ratio of seven ring protons/1 aromatic amine protons.

3.2. Synthesis and characterization of HBP-g-silica

Organic/inorganic conjugation was examined in HBP-g-silica. The FT-IR spectroscopy was used to identify the presence of related bond with inorganic materials Fig. 3. The band at 1630 cm^{-1} is due to amid I band (C=O stretch) [22,23]. Relatively strong bending band is shown at around 1550 cm^{-1} for secondary amide structure due to its combination of C–N stretching band and its N–H bending band [24]. Also, the band at 3,180, 3,350 cm^{-1} suggested the formation of amide bond which is caused by the grafted PA polymer onto HBP-g-silica. The presence of HBP-g-silica is reflected as a strong band at about 670, 740, and 1,060–1,080 cm^{-1}. These results verify that PA chains from HBP were chemically grafted onto the HBP-g-silica surface.

3.3. Properties of membrane

The FT-IR spectroscopy was used to identify the presence of functional groups in the active layer of TFC membranes.

In Fig. 4, there are various peaks of aPAM, H-aPAM and PAM membranes. There are only few peaks and small transmittance in the PAM spectrum. The peaks examine chemical bonding at 1663 cm^{-1} amid I band (C=O stretching—dominant contributor, C–N stretching, and C–C–N deformation vibration in a secondary amide group), at 1,609 cm^{-1} aromatic amide (N–H) deformation vibration and C=C ring stretching vibration, at 1,550 cm^{-1} amid II band (N–H in-plane bending and N–C stretching vibration of a –CO–NH– group) and for semi-aromatic poly(piperazinamide), at 1,630 cm^{-1} amid I band for poly(piperaz-

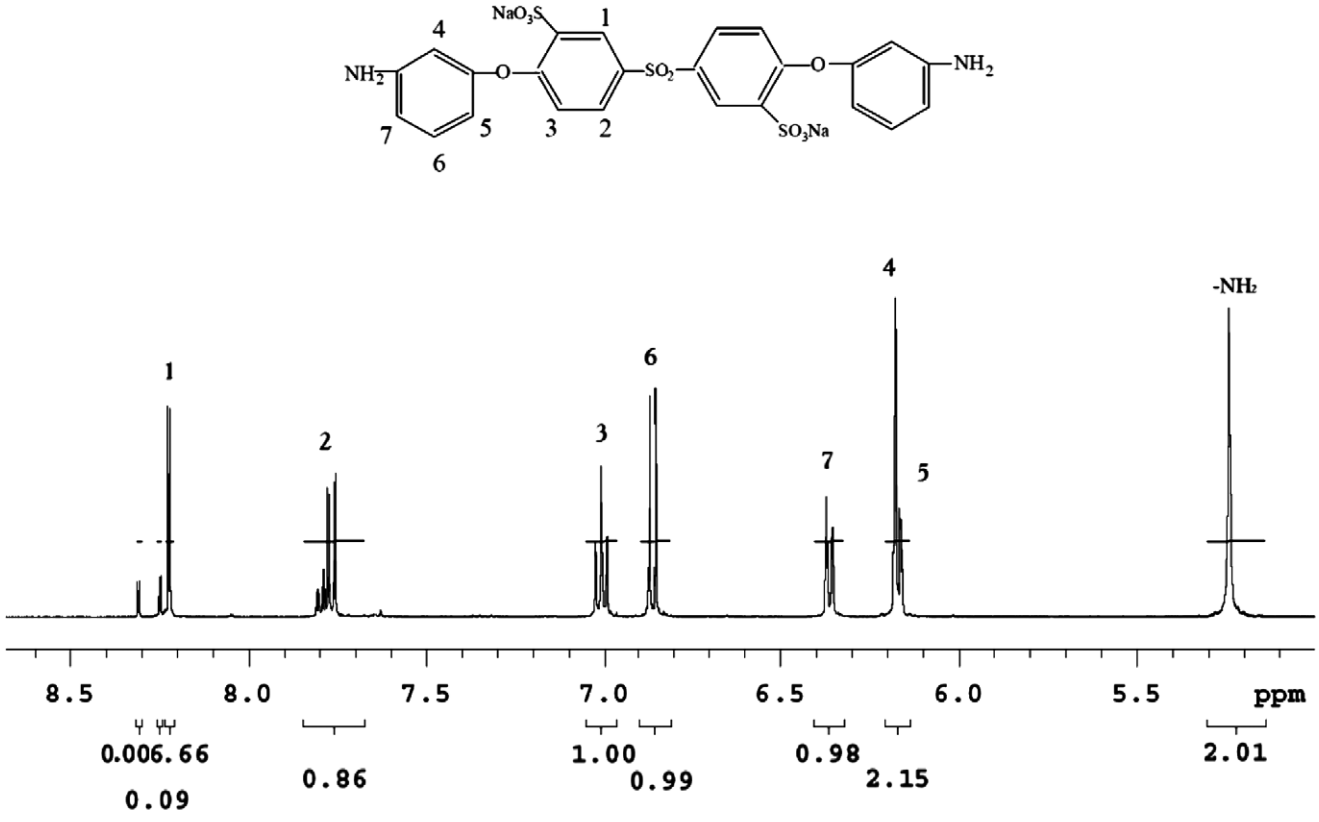

Fig. 2. ^{1}H-NMR spectra of aPES in DMSO-d_6.

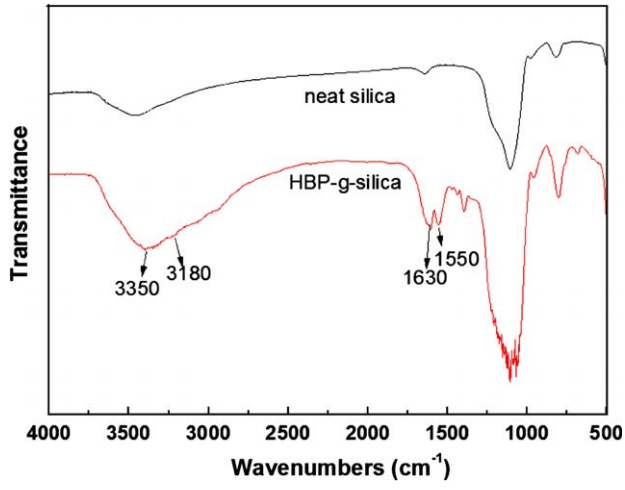

Fig. 3. The FT-IR spectra of neat silica and HBP-g-silica.

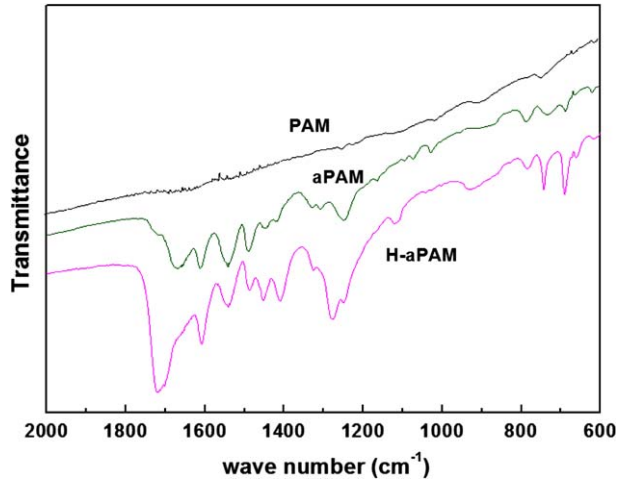

Fig. 4. The FT-IR spectra of PAM, aPAM, and H-aPAM.

inamide) in aPAM and H-aPAM FT-IR spectra [22–25]. A linear relationship exists between the degree of sulfonation and the density ratio of sulfonate stretching at 1,030 cm^{-1} to diphenyl ether band at 1,006 cm^{-1}. The presence of HBP-g-silica is well reflected as a strong band at 670, 740, and 1,060–1,080 cm^{-1}. Thus, the FT-IR spectra confirm that HBP-g-silica was chemically combined with copolymer in the H-aPAM active layer. The presence of HBP-g-silica may change the matrix of active layer into a firm and complex structure on the RO membrane.

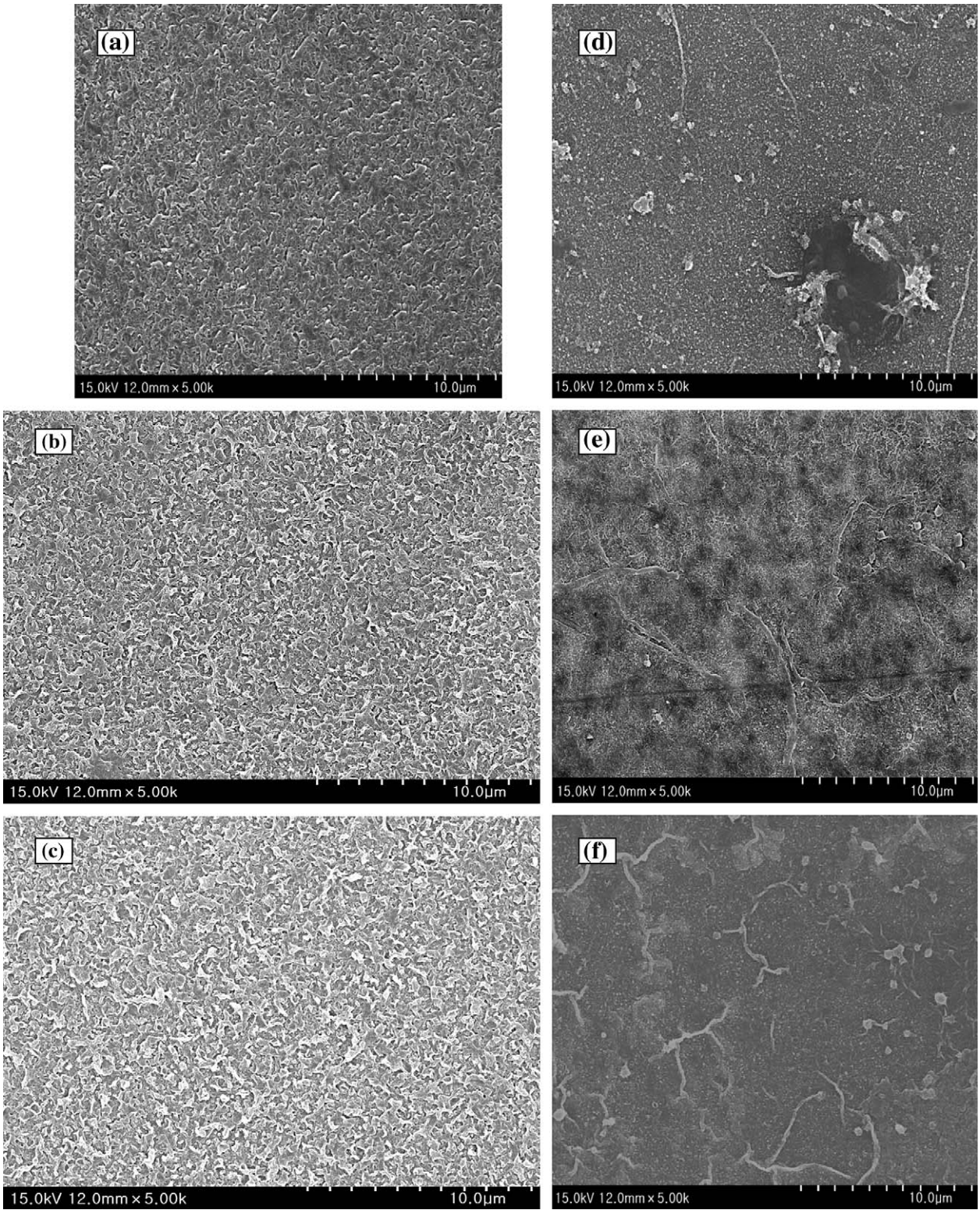

Fig. 5. SEM images of surface of fresh PAM (a), aPAM (b), and H-aPAM (c) before chlorination, and surface of PAM (d), aPAM (e), and H-aPAM (f) after chlorination.

3.4. Membrane surface structure

Surface morphological structure of the composite membranes before and after chlorination condition was characterized by using SEM. SEM images of the fresh and chlorinated membrane surface for PAM, aPAM, and H-aPAM are provided in Fig. 5. Fig. 5(a) shows that the surface feature of the fresh PAM appears regular and with packed patterns, while the surface feature of aPAM and H-aPAM in Fig. 5(b) and (c) appears to be infrequently and irregularly. The microscale surface morphology of H-aPAM shows three-dimensional structures due to steric conformation with HBP-g-silica particles. After chlorination, the surfaces of membranes are flat and smooth due to the degradation of copolymer matrix. The round and large defects appeared on PAM of Fig. 5(d), while the linear and thin defects appeared on aPAM of Fig. 5(e). The surface feature of H-aPAM in Fig. 5(f) becomes denser and compacter than others, and the degradable copolymer is sparsely dotted with HBP-g-silica particles.

3.5. Effect HBP-g-silica on chlorine toleranance of RO membrane

RO performance in Fig. 6 in terms of water flux and salt rejection was evaluated using the PAM, aPAM, and H-aPAM before and after chlorination through cross-flow permeation tests. The test conditions were the same as the actual desalination process conditions, 32 g/L NaCl concentration and 55 bar pressure. The performance of RO membranes fluctuated in the beginning of the measurement, but it reached a steady state after 2 h. The measured water flux and salt rejection of membranes chlorinated under conditions of 500 mg/l NaOCl for 24 h is presented in Fig. 6

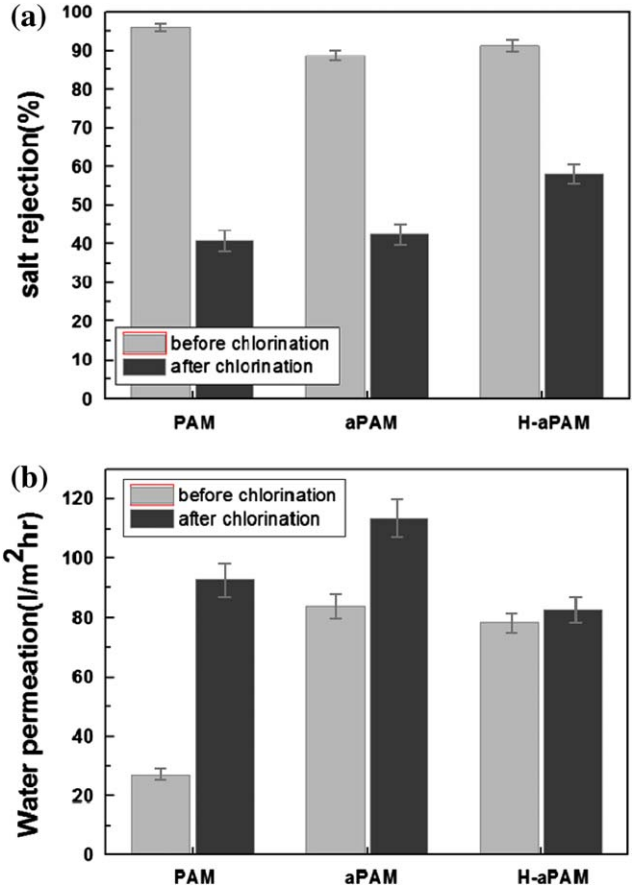

Fig. 6. The performance of self-made RO membranes: (a) salt rejection and (b) water permeation.

(b). After chlorination, the lower performance of membranes resulted from flow through a lot of defects and large pores in all membranes' surface. The salt rejection of chlorinated aPAM is reduced by 52%, while the salt rejection decreases from 95.9% for the fresh

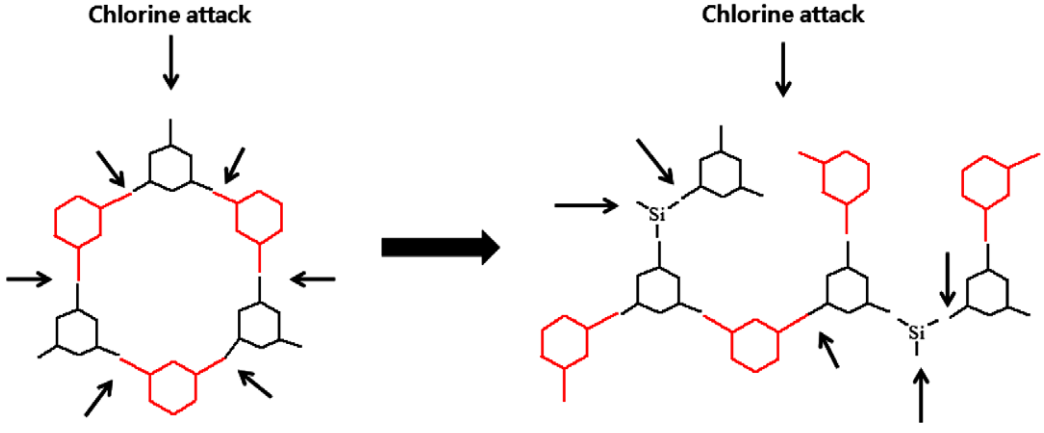

Fig. 7. The mechanism of chlorine attack on the RO membrane active layer.

PAM to 40.6% after chlorination. The water permeation of chlorinated aPAM and PAM increases to 34% and 242% when compared to values before chlorination, respectively. The N-chlorination and concomitant ring-chlorination reactions through Orton-rearrangement can disrupt the intermolecular hydrogen bonds and destroy the symmetry of polyamide network, sequentially resulting in a transformation from crystalline regions to an amorphous state [26–28]. Fig. 6 clearly shows that the chlorine resistance of the H-PAM is much better than that of the aPAM, PAM. The good chlorine resistance of the H-aPAM can be explained as follows. HBP-g-silica was chemically combined with copolymer in the H-aPAM active layer. The intermolecular hydrogen bonding is enhanced by the coating layer [29]; this will impede the replacement of hydrogen with chlorine on the amide groups of the aromatic polyamide membranes [26]. The presence of HBP-g-silica may change the matrix of active layer into compacted and complex structure with steric conformation. Furthermore, amino groups in HBP-g-silica and TMC are combined through the formation of an amide bond in the RO membrane active layer. These additional amide bonds and unreacted amino groups of HBP-g-silica protected the active layer from chlorine. The scheme of simplified mechanism of chlorine attack on the active layer is shown in Fig. 7.

The protective and sacrificial composition between HBP-g-silica and copolymer will prevent the attack of chlorine on the underlying active layer.

4. Conclusion

The chlorine-tolerance of HBP-g-silica and aPES composite polyamide membrane has been presented. The FT-IR spectra of HBP-g-silica showed that amine groups were grafted onto the silica surface and amide bonds were conjugated between PA and HBP-g-silica. The PAM, aPAM, and H-aPAM were fabricated by interfacial polymerization. The different properties of membranes were characterized by FT-IR spectra and SEM to verify effectiveness of HBP-g-silica. The performance of H-aPAM was evaluated to exhibit 91.2% salt rejection and 78.34 L/m^2 water permeation. After chlorination, H-aPAM shows lower decrease in 36% of salt rejection and increase in 5% of water permeation than PAM. The HBP-g-silica loading significantly modified the three-dimensional PA network structure and contributed to high performance by the chain stiffness of the copolymer and high degree of cross-linking.

Acknowledgments

This research was supported by a Grant (#11 seaHERO B02-06) from Plant Technology Advancement Program funded by the Ministry of Land, Transport and Maritime Affairs of the Korean government and the Human Resources Development; the Korea Institute of Energy Technology Evaluation and Planning (20114010203050) grant funded by the Korea government Ministry of Knowledge Economy.

References

[1] D. Li, H. Wang, Recent developments in reverse osmosis desalination membranes, J. Mater. Chem. 20 (2010) 4551–4566.
[2] W.J. Lau et al., A recent progress in thin film composite membrane: A review, Desalination 287 (2012) 190–199.
[3] C.Y. Tang, Y.N. Kwon, J.O. Leckie, Probing the nano- and micro-scales of reverse osmosis membranes—A comprehensive characterization of physiochemical properties of uncoated and coated membranes by XPS, TEM, ATR-FTIR, and streaming potential measurements, J. Membr. Sci. 287 (2007) 146–156.
[4] G.L. Jadav, P.S. Singh, Synthesis of novel silica—polyamide nano composite membrane with enhanced properties, J. Membr. Sci. 328 (2009) 257–267.
[5] M. Liu, D. Wu, S. Yu, C. Gao, Influence of the polyacyl chloride structure on the reverse osmosis performance, surface properties and chlorine stability of the thin-film composite polyamide membranes, J. Membr. Sci. 326 (2009) 205–214.
[6] B. Tang, C. Zou, P. Wu, Study on a novel polyester composite nanofiltration membrane by interfacial polymerization. II. The role of lithium bromide in the performance and formation of composite membrane, J. Membr. Sci. 365 (2010) 276–285.
[7] G. Chen, S. Li, X. Zhang, S. Zhang, Novel thin-film composite membranes with improved water flux from sulfonated cardo poly(arylene ether sulfone) bearing pendant amino groups, J. Membr. Sci. 310 (2008) 102–109.
[8] H. Wang, L. Li, X. Zhang, S. Zhang, Polyamide thin-film composite membranes prepared from a novel triamine 3,5-diamino-N-(4-aminophenyl)-benzamide monomer and m-phenylenediamine, J. Membr. Sci. 353 (2010) 78–84.
[9] H.S. Lee, S.J. Im, J.H. Kim, J.P. Kim, B.R. Min, Polyamide thin film nanofiltration membranes containing TiO_2 nanoparticles, Desalination 219 (2008) 48–56.
[10] H. Wu, B. Tang, P. Wu, MWNTs/polyester thin film nanocomposite membrane: An approach to overcome the trade-off effect between permeability and selectivity, J. Phys. Chem. C 114 (2010) 16395–16400.
[11] H. Zou, Y. Jin, J. Yang, H. Dai, X. Yu, J. Xu, Synthesis and characterization of thin film composite reverse osmosis membranes via novel interfacial polymerization approach, Sep. Purif. Technol. 72 (2010) 256–262.
[12] S. Verssimo, K.V. Peinemann, J. Bordado, New composite hollow fiber membrane for nanofiltration, Desalination 184 (2005) 1–11.
[13] C. Brousse, R. Chapurlat, J.P. Quentin, New membranes for reverse osmosis I. Characteristics of the base polymer: Sulphonated polysulphones, Desalination 18 (1976) 137–153.
[14] C.W. Plummer, G. Kimura, A.B. La Conti, NTIS Report No. PB-201034, 1970.
[15] B.C. Johnson, İ. Yilgör, C. Tran, M. Iqbal, J.P. Wightman, D.R. Lloyd, J.E. McGrath, Synthesis and characterization of sulfonated poly(acrylene ether sulfones), J. Polym. Sci. Polym. Chem. Ed. 22 (1984) 721–737.

[16] Y. Li, F. Wang, J. Yang, D. Liu, A. Roy, S. Case, J. Lesko, J. McGrath, Synthesis and characterization of controlled molecular weight disulfonated poly(arylene ether sulfone) copolymers and their applications to proton exchange membranes, Polymer 47 (2006) 4210–4217.
[17] G.M. Geise, H.-S. Lee, D.J. Miller, B.D. Freeman, J.E. McGrath, D.R. Paul, Water purification by membranes: The role of polymer science, J. Polym. Sci. Part B: Polym. Phys. 48 (2010) 1685–1718.
[18] M. Paul et al., Synthesis and crosslinking of partially disulfonated poly(arylene ether sulfone) random copolymers as candidates for chlorine resistant reverse osmosis membranes, Polymer 49 (2008) 2243–2252.
[19] F. Wang, M. Hickner, Y.S. Kim, T.A. Zawodzinski, J.E. McGrath, Direct polymerization of sulfonated poly(arylene ether sulfone) random (statistical) copolymers: Candidates for new proton exchange membranes, J. Membr. Sci. 197 (2002) 231.
[20] F. Wang, J.E. McGrath, Synthesis of Poly(arylene ether)s. Synthesis Methods in Step-Growth Polymers, John, New York, NY, 2003.
[21] M.A. Hickner, H. Ghassemi, Y.S. Kim, B.R. Einsla, J.E. McGrath, Alternative polymer systems for proton exchange membranes (PEMs), Chem. Rev. 104 (2004) 4587.
[22] Y.N. Kwon, J.O. Leckie, Hypochlorite degradation of crosslinked polyamide membranes II. Changes in hydrogen bonding behavior and performance, J. Membr. Sci. 282 (2006) 456–464.
[23] D.J. Skrovanek, S.E. Howe, P.C. Painter, M.M. Coleman, Hydrogen-bonding in polymers—infrared temperature studies of an amorphous polyamide, Macromolecules 18 (1985) 1676.
[24] S. Wu, G. Zheng, H. Lian, J. Xing, L. Shen, Chlorination and oxidation of aromatic polyamides. I. Synthesis and characterization of some aromatic polyamides, J. Appl. Polym. Sci. 61 (1996) 415–420.
[25] N.W. Oh, J. Jegal, K.H. Lee, Preparation and characterization of nanofiltration composite membranes using polyacrylonitrile (PAN). II. Preparation and characterization of polyamide composite membranes, J. Appl. Polym. Sci. 80 (2001) 2729.
[26] M. Liu et al., Thin-film composite polyamide reverse osmosis membranes with improved acid stability and chlorine resistance by coating N-isopropylacrylamide–co-acrylamide copolymers, Desalination 270 (2011) 248–257.
[27] G.D. Kang, C.J. Gao, W.D. Chen, X.M. Jie, Y.M. Cao, Q. Yuan, Study on hypochlorite degradation of aromatic polyamide reverse osmosis membrane, J. Membr. Sci. 300 (2007) 165–171.
[28] Y.-N. Kwon, J.O. Leckie, Hypochlorite degradation of crosslinked polyamide membranes. II. Changes in hydrogen bonding behavior and performance, J. Membr. Sci. 282 (2006) 456–464.
[29] D. Wu, X. Liu, S. Yu, M. Liu, C. Gao, Modification of aromatic polyamide thin-film composite reverse osmosis membranes by surface coating of thermo-responsive copolymers P (NIPAM-co-Am) I: Preparation and characterization, J. Membr. Sci. 352 (2010) 76–85.